ARTICLE
Journal of Cellular Biochemistry 110:609–619 (2010)

Journal of Cellular Biochemistry

PR-Set7-Mediated Monomethylation of Histone H4 Lysine 20 at Specific Genomic Regions Induces Transcriptional Repression

Lauren M. Congdon, Sabrina I. Houston, Chendhore S. Veerappan, Tanya M. Spektor, and Judd C. Rice*

Department of Biochemistry and Molecular Biology, University of Southern California Keck School of Medicine, Los Angeles, California 90033

ABSTRACT

Increasing evidence indicates that the post-translational modifications of the histone proteins play critical roles in all eukaryotic DNA-templated processes. To gain further biological insights into two of these modifications, the mono- and trimethylation of histone H4 lysine 20 (H4K20me1 and H4K20me3), ChIP-chip experiments were performed to identify the precise genomic regions on human chromosomes 21 and 22 occupied by these two modifications. Detailed analysis revealed that H4K20me1 was preferentially enriched within specific genes; most significantly between the first ~5% and 20% of gene bodies. In contrast, H4K20me3 was preferentially targeted to repetitive elements. Among genes enriched in H4K20me3, the modification was typically targeted to a small region ~1 kb upstream of transcription start. Our collective findings strongly suggest that H4K20me1 and H4K20me3 are both physically and functionally distinct. We next sought to determine the role of H4K20me1 in transcription since this has been controversial. Following the reduction of PR-Set7/Set8/KMT5a and H4K20me1 in cells by RNAi, all H4K20me1-associated genes analyzed displayed an ~2-fold increase in gene expression; H4K20me3-associated genes displayed no changes. Similar results were obtained using a catalytically dead dominant negative PR-Set7 indicating that H4K20me1, itself, is essential for the selective transcriptional repression of H4K20me1-associated genes. Furthermore, we determined that the H4K20me1-associated DNA sequences were sufficient to nucleate H4K20me1 and induce repression in vivo. Our findings reveal the molecular mechanisms of a mammalian transcriptional repressive pathway whereby the DNA sequences within specific gene bodies are sufficient to nucleate the monomethylation of H4K20 which, in turn, reduces gene expression by half. J. Cell. Biochem. 110: 609–619, 2010.

KEY WORDS: HISTONE H4; METHYLATION; PR-Set7; TRANSCRIPTIONAL REGULATION; CHROMATIN

The fundamental subunit of eukaryotic chromatin is the nucleosome, which consists of 146 bp of DNA wrapped around an octamer of the core histones proteins H2A, H2B, H3, and H4. Due to their strong association with DNA, it has long been postulated that histones play a vital role in most, if not all, DNA-templated processes [Strahl and Allis, 2000]. Research over the last few decades has revealed that these distinct biological programs are intimately correlated with the specific covalent post-translational modifications of histones including acetylation, phosphorylation, and methylation [Jenuwein and Allis, 2001]. Our current understanding of the role of histone modifications in chromatin structure, function, and dynamics has largely been shaped by the technological breakthrough of chromatin immunoprecipitation (ChIP) [Kuo and Allis, 1999]. In this method, select regions of the genome are isolated by immunoprecipitation using an antibody that recognizes a specific histone modification or other DNA-associated factor. Several recent studies have combined the power of ChIP with high-throughput technologies, including DNA genome tiling microarrays (ChIP-chip) and large capacity direct DNA sequencers (ChIP-Seq), to determine the precise genomic locations of various histone modifications and transcription factors [Bernstein et al., 2005; Boyer et al., 2005, 2006; Barski et al., 2007]. The vast majority of these genome-wide studies focused on factors and histone modifications associated with transcriptional initiation and elongation [Guenther

Lauren M. Congdon, Sabrina I. Houston, and Chendhore S. Veerappan contributed equally to this work.

Additional Supporting Information may be found in the online version of this article.

Grant sponsor: National Institutes of Health; Grant number: GM075094; Grant sponsor: Pew Charitable Trusts; Grant sponsor: Donald E. and Delia B. Baxter Foundation; Grant sponsor: Robert E. and May R. Wright Foundation.

*Correspondence to: Dr. Judd C. Rice, Department of Biochemistry and Molecular Biology, University of Southern California Keck School of Medicine, 1450 Biggy Street, NRT 6506, Los Angeles, CA 90033. E-mail: juddrice@usc.edu

Received 13 September 2009; Accepted 3 February 2010 • DOI 10.1002/jcb.22570 • © 2010 Wiley-Liss, Inc.
Published online 1 April 2010 in Wiley InterScience (www.interscience.wiley.com).

et al., 2007; Heintzman et al., 2007; Mikkelsen et al., 2007]. These findings have dramatically improved our fundamental understanding of transcription and transcriptional regulation in a very short time.

Although histone H4 lysine 20 (H4K20) methylation was one of the first post-translationally modified histone residues to be discovered, the biological importance of this histone modification is only now beginning to emerge [Murray, 1964]. H4K20 can be mono-, di-, or trimethylated in vivo and all three methylated forms are evolutionarily conserved from *Schizosaccharomyces pombe* to man [Sims et al., 2006; Sautel et al., 2007; Yang and Mizzen, 2009]. In *S. pombe*, the Set9/KMT5 enzyme mediates all three forms of methylation and these modifications have been linked to DNA damage repair by binding the Crb2 repair protein at sites of damage [Sanders et al., 2004]. In contrast to yeast, recent findings indicate that different methylated forms of H4K20 are created by distinct enzymes in higher eukaryotes. In metazoans, the Suv4-20h1/KMT5b and Suv4-20h2/KMT5c enzymes are responsible for the bulk of di- and trimethylation (H4K20me2 and H4K20me3) [Schotta et al., 2004; Sakaguchi et al., 2008]. Similar to yeast, H4K20me2 has been implicated in DNA repair by binding the 53BP1 repair protein at damaged foci [Botuyan et al., 2006; Yang et al., 2008]. In contrast, H4K20me3 appears to be functionally linked with trimethylated histone H3 lysine 9 in the establishment and maintenance of pericentric heterochromatin [Schotta et al., 2004]. Mice lacking both Suv4-20 enzymes display global reductions of H4K20me2 and H4K20me3, defects in DNA damage repair, increased chromosomal aberrations and perinatal lethality [Schotta et al., 2008].

The PR-Set7/Set8/KMT5a enzyme is the only known enzyme that specifically monomethylates histone H4 lysine 20 (H4K20me1) [Couture et al., 2005; Xiao et al., 2005]. In contrast to the other H4K20 methylated forms, the precise biological role(s) of H4K20me1 is(are) far less clear. However, these unknown roles are essential as the loss of PR-Set7 and H4K20me1 results in DNA damage, defects in chromatin condensation, chromosomal segregation defects, and early embryonic lethality prior to the eight-cell stage [Nishioka et al., 2002; Sakaguchi and Steward, 2007; Houston et al., 2008; Huen et al., 2008; Oda et al., 2009]. One role for H4K20me1 appears to be its involvement in the cell cycle; however, it remains unclear when it functions (S-phase and/or G2/M) and exactly what its function is [Rice et al., 2002; Jorgensen et al., 2007; Pesavento et al., 2007; Tardat et al., 2007; Houston et al., 2008]. Another role for H4K20me1 is in transcriptional regulation where it was originally found associated with transcriptionally repressed chromatin and, consistent with this, was later found to play a putative role in X chromosome inactivation [Fang et al., 2002; Nishioka et al., 2002; Kohlmaier et al., 2004; Karachentsev et al., 2005]. However, recent reports demonstrate that H4K20me1 is detected within active genes suggesting a role for H4K20me1 in promoting transcription [Talasz et al., 2005; Vakoc et al., 2006; Barski et al., 2007]. These contradictory findings indicate that the precise role of H4K20me1 in transcriptional regulation remains unknown.

The goal of this study was to clarify the role of H4K20me1 in transcriptional regulation by identifying and analyzing endogenous human H4K20me1-associated genes. Since these were unknown, ChIP-chip was employed to accurately determine these genes on human chromosomes 21 and 22 followed by detailed analysis of their expression profiles in the absence of PR-Set7 and H4K20me1. Our findings demonstrate that H4K20me1 is significantly enriched within the first half of gene bodies of specific genes. We also found that these H4K20me1-associated DNA sequences were sufficient to nucleate H4K20me1 in vivo. Furthermore, we found that H4K20me1, itself, was required for the transcriptional repression of all H4K20me1-associated genes analyzed regardless of their basal expression status. Although H4K20me3 was used as a negative control in these studies, we serendipitously discovered that it may also have undefined roles in transcriptional regulation of specific genes. Collectively, our findings elucidate the molecular mechanisms of a novel H4K20me1-dependent mammalian gene-silencing pathway.

MATERIALS AND METHODS

CHROMATIN IMMUNOPRECIPITATION (ChIP)

HeLa or HEK 293 cells were fixed in 1% formaldehyde for 10 min before quenching with 0.125 M glycine for 5 min. Nuclei were isolated using nuclear isolation buffer (150 mM NaCl, 10 mM HEPES, pH 7.5, 1.5 mM $MgCl_2$, 10 mM KCl, 0.5% NP-40, 0.5 mM DTT) and resuspended in nuclear lysis buffer (50 mM Tris–HCl, pH 8.1, 10 mM EDTA, 1% SDS) at a concentration of 10^8 nuclei per ml. Nuclei were sonicated to DNA fragments ranging from 200 to 600 bp. For each ChIP, sonicated nuclear material from 5×10^6 cells was immunoprecipitated with either rabbit IgG, a Histone H3 general antibody (Abcam, Ab1791 Lot #172452), a histone H4K20me1-specific (Active Motif, #39175), a histone H4K20me3-specific antibody (Active Motif, #39180), or a FLAG antibody (Sigma, #F7425 Lot #096K4803). Immune complexes were precipitated with Protein-A-conjugated sepharose (Amersham, GE Biosciences) and washed with RIPA buffer (50 mM HEPES, pH 7.4, 1 mM EDTA, 1% NP-40, 0.7% sodium deoxycholate, 500 mM LiCl). DNA was eluted using 10% Chelex (Bio-Rad) solution [Nelson et al., 2006].

ChIP-Chip AND ChIP-CLONING

The ChIPed material above was linker-ligated and PCR amplified using the oligoJW102 and oligoJW103 primers (Supplemental Table V). Four micrograms of PCR amplified DNA was sent to NimbleGen Corporation for Cy3/Cy5 labeling, array hybridization, and data collection. Three independent biological replicates were performed for both monomethylated and trimethylated H4K20. This material was also ligated into the pGEM-T-Easy TA cloning vector (Promega), transformed into *E. coli*, and insert-positive clones were directly sequenced [Weinmann and Farnham, 2002].

PEAK DETECTION AND GENE IDENTIFICATION

The *.gff* files (http://www.histonecode.com) generated by NimbleGen were used to determine sites of H4K20me1 and H4K20me3 enrichment using the freely available software, *M*odel-based *A*nalysis of *2*-Color arrays (MA2C) [Song et al., 2007]. Two channel data from the input and ChIP sample were loaded into the program. Default parameters were used to determine peaks with a *P*-value threshold of 0.005 or 0.001. The *.gff* files were converted to *.bed* files

and, along with the peaks detected by MA2C, were visualized using the HG18 version of the human genome on the UCSC genome browser [Karolchik et al., 2008]. Gene annotation files were downloaded from the NimbleGen website and a panel of genes containing at least one statistically significant peak ($P < 0.005$) for H4K20me1 or H4K20me3 within the gene body, or within a 5 kb region 5′ upstream or a 500 bp region 3′ downstream of the gene, were identified. The H4K20-methyl peak density for each gene was determined by dividing the length of the peak by the gene length (Supplemental Tables III and IV).

PEAK DISTRIBUTION ANALYSIS

To characterize the average distribution of H4K20me1 and H4K20me3 peaks in the promoter and 3′ flanking region of modification positive genes, the cumulative number of peaks per nucleotide position was first determined. To analyze the peak distribution within the genes, each H4K20me-positive gene body was divided into 1/10,000th in order to normalize for differences in gene lengths; the number of peaks within each fraction was summed. The peak numbers were converted to tag density values by dividing the cumulative peak count for each nucleotide or gene body fraction by the total peak numbers from all H4K20me1 or H4K20me3-positive genes (y-axis). Tag density values were analyzed using a Poisson distribution with λ equal to the average tag density value (gray line) in order to determine statistically significant ($P < 0.05$) regions of H4K20me1 or H4K20me3 enrichment (black bars).

GENE EXPRESSION ANALYSIS

Lipofectamine 2000 (Invitrogen) was used to transfect HeLa cells with pSUPERIOR.retro.puro vectors (OligoEngine) producing either a functional or non-functional shRNA for PR-Set7 [Houston et al., 2008]. Positive cells were selected by adding 4 μg/ml of puromycin 24 h following transfection. A Qiagen RNeasy Kit was used to isolate total RNA from cells 6 days post-transfection when PR-Set7 depletion was observed by Western analysis. RNA was converted to cDNA using the ABI Reverse Transcription Kit according to the manufacturer's instructions. Quantitative real-time PCR was performed with SYBR Green (Bio-Rad) using a Bio-Rad I-Cycler. Expression was normalized to *MTMR3* expression levels which were unaltered in all samples (Supplemental Fig. 1). Lipofectamine 2000 was also used to transfect HeLa cells with either the pQCXIP empty vector (Clontech) or the vector expressing a full-length PR-Set7 R265G point mutant [Sims and Rice, 2008]. Following puromycin selection, total RNA was isolated for analysis 4 days post-transfection when depletion of monomethylated H4K20 was observed by Western analysis. Three independent biological replicates were performed to generate standard deviation. The Student's t-test was used to determine statistical significance. All primer sets and PCR conditions are detailed in Supplemental Table V and were verified to be in the linear range of amplification.

pTK-Luc2 LUCIFERASE ASSAYS

H4K20me1-positive and -negative regions were cloned into the pTK-Luc2 plasmid using primer sets detailed in Supplemental Table V. Lipofectamine 2000 (Invitrogen) was used to co-transfect HEK 293 cells in six-well plates with 4 μg of each pTK-luc2 construct and 5 ng of the pRL-CMV (Promega) control plasmid according to the manufacturer's instructions. Cells were harvested 48 h post-transfection and luciferase assays were performed using a Dual-Luciferase Reporter Assay Kit (Promega). Luciferase expression of each pTK-luc2 construct was normalized to Renilla expression. Three independent biological replicates were performed to generate standard deviation.

RESULTS

ChIP-Chip REVEALS SPECIFIC REGIONS OF H4K20me1 AND H4K20me3 ENRICHMENT ON HUMAN CHROMOSOMES 21 AND 22

By using a novel panel of modification-specific antibodies that can discriminate between the different methylated forms of histone H4K20 in indirect immunofluorescence microscopy studies, we previously demonstrated that H4K20me1 is selectively targeted to distinct transcriptionally silent nuclear compartments in the mammalian genome while the majority of H4K20me3 is targeted to pericentric heterochromatin [Sims et al., 2006]. In contrast, H4K20me2 is present in >80% of H4 molecules and is dispersed ubiquitously throughout the genome [Pesavento et al., 2007]. To determine the precise genomic locations of H4K20me1 and H4K20me3 at high resolution, the same antibodies were used in ChIPs to isolate regions of the HeLa genome enriched in these histone modifications. The purified H4K20me1 and H4K20me3-associated DNA was blunted, PCR amplified, labeled, and hybridized to a NimbleGen oligonucleotide genome tiling microarray containing the entire length of human chromosomes 21 and 22 and a small portion of the X chromosome, with input DNA used for reference of enrichment. This design allowed for the unbiased interrogation of two whole human chromosomes on a single microarray chip at 100 bp resolution.

Currently, there are various computational methods to identify regions, or "peaks," of enrichment for histone modifications and transcription factors on genome tiling arrays. While several of these methods limit their analysis to only individual oligonucleotide probes rather than a region of the genome, other programs take into account a neighboring effect of nearby probes to aid in peak identification. We employed one such program, called MA2C [Song et al., 2007], to detect peaks of H4K20me1 and H4K20me3 enrichment using the log 2 ratios of ChIP DNA versus the input genomic DNA and accounting for GC-content bias in the probes. In all cases, MA2C consistently provided robust and visually verifiable peaks resulting in the identification of 359 statistically significant ($P < 0.005$) regions enriched in H4K20me1 on human chromosomes 21 and 22 (162 peaks at $P < 0.001$) (Table I). For H4K20me3, 426 significant ($P < 0.005$) peaks were identified by MA2C (195 peaks at $P < 0.001$).

H4K20me1 IS PREFERENTIALLY ENRICHED IN GENE BODIES WHEREAS THE MAJORITY OF H4K20me3 IS FOUND IN REPETITIVE ELEMENTS

Analysis of the H4K20me1 peaks identified by MA2C revealed that this histone modification is preferentially enriched within the body of genes (75%) (Fig. 1A). In contrast, the majority of the H4K20me3

TABLE I. MA2C Analysis of ChIP-Chip Data Sets Identifies H4K20me1- and H4K20me3-Associated Peaks and Genes on HeLa Chromosomes 21 and 22

Modification	Significance	Total no. of peaks	No. of genes with peaks	No. of peaks within genes
H4K20me1	$P < 0.005$	359	156	275
	$P < 0.001$	162	83	124
H4K20me3	$P < 0.005$	426	142	197
	$P < 0.001$	195	73	89

peaks were detected in intergenic regions (54%). There were more H4K20me3 peaks detected (6%) than H4K20me1 peaks (2%) in the regions proximal to genes (5 kb upstream or 500 bp downstream). These data strongly suggest that H4K20me1 is specifically targeted to genes compared to H4K20me3.

Since repetitive elements are excluded from genome tiling arrays, it remained a distinct possibility that H4K20me1 and H4K20me3 were also targeted to certain repetitive elements. To investigate this possibility, the ChIPs for H4K20me1 and H4K20me3 were repeated and the enriched DNA was used to create small bacterial libraries for direct sequencing (ChIP-cloning) [Weinmann and Farnham, 2002]. Due to the abundance of repetitive elements in the human genome, we reasoned that if H4K20me1 or H4K20me3 were targeted to these elements then the vast majority of the sequences would contain repeats. However, out of the 86 H4K20me1 ChIP sequences (Supplemental Table I), nearly half (42%) corresponded to non-repetitive elements (Fig. 1B). In contrast, the majority (77%) of the 57 H4K20me3 ChIP clones contained repetitive sequences (Supplemental Table II); most of these were SINE elements (43%). These findings indicate that H4K20me3 is preferentially enriched within repetitive elements, whereas H4K20me1 is typically enriched within gene bodies.

H4K20me1 AND H4K20me3 ARE TYPICALLY TARGETED TO DIFFERENT GENES

The H4K20me1 and H4K20me3 ChIP-chip data were mapped to the human genome using the UCSC genome browser to identify the peak-associated genes and determine their general peak characteristics within the gene body and proximal regions (5 kb upstream and downstream). The mapping of the 359 statistically significant ($P < 0.005$) H4K20me1 peaks revealed that >76% of the peaks (275)

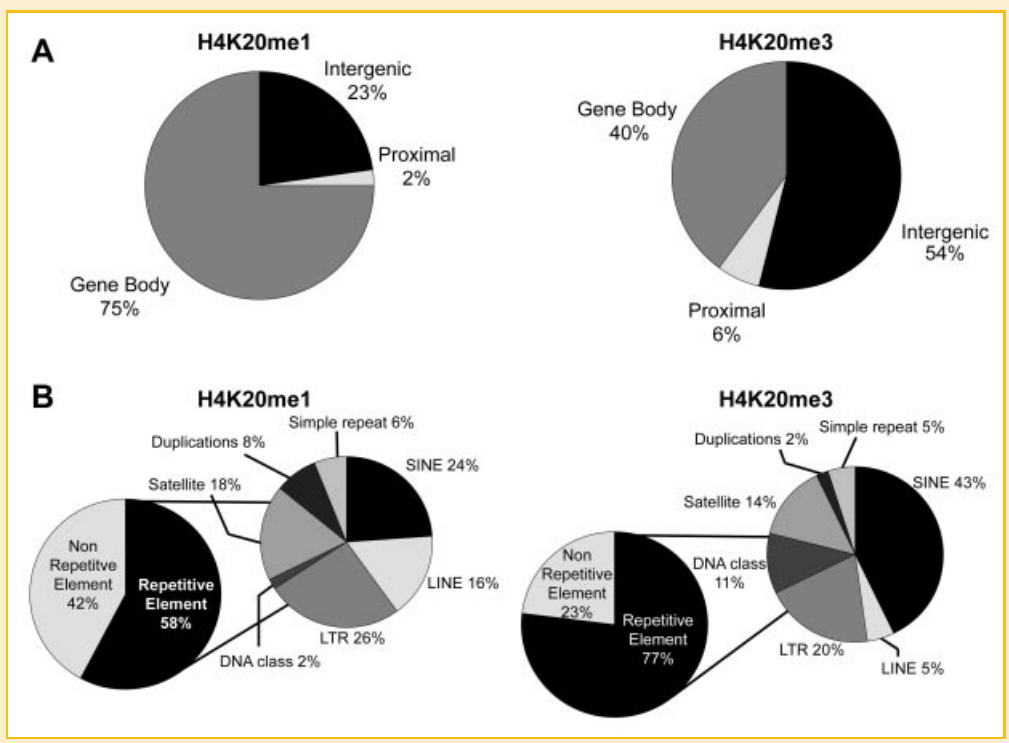

Fig. 1. H4K20me1 is preferentially enriched within genes while H4K20me3 is typically located within repetitive elements. A: Chromatin immunoprecipitations (ChIPs) were performed in HeLa cells to isolate H4K20me1- and H4K20me3-associated DNA. The ChIPed material was hybridized to a NimbleGen oligonucleotide genome tiling microarray containing the entire length of human chromosomes 21 and 22. Statistically significant peaks ($P < 0.005$) of enrichment were identified using MA2C software. The percentages of peaks located in specific genomic regions are represented. Proximal is defined as the regions 5 kb upstream and 500 bp downstream of the gene body. B: ChIPed material was cloned and 86 insert positive H4K20me1-associated clones and 57 H4K20me3-associated clones were directly sequenced. The general distribution of the sequences and the different classes of corresponding repetitive elements are shown.

were found within 156 genes (Table I). By increasing the stringency of the analysis ($P < 0.001$), we consistently found that >76% of the 162 identified H4K20me1 peaks (124) were found within 83 genes (Supplemental Table III). Similar analysis was conducted to determine H4K20me3-associated genes. In contrast to H4K20me1, the mapping of the 426 statistically significant ($P < 0.005$) H4K20me3 peaks revealed that <47% of the peaks (197) were found within a total of 142 genes. Similarly, only <47% (89) of the 195 H4K20me3 peaks detected at $P < 0.001$ were found within 73 genes (Supplemental Table IV). This approach has led to the identification of specific genes on human chromosomes 21 and 22 enriched in H4K20me1 and H4K20me3.

We next sought to determine if H4K20me1 and H4K20me3 tended to be present within the same genes or if they were targeted to

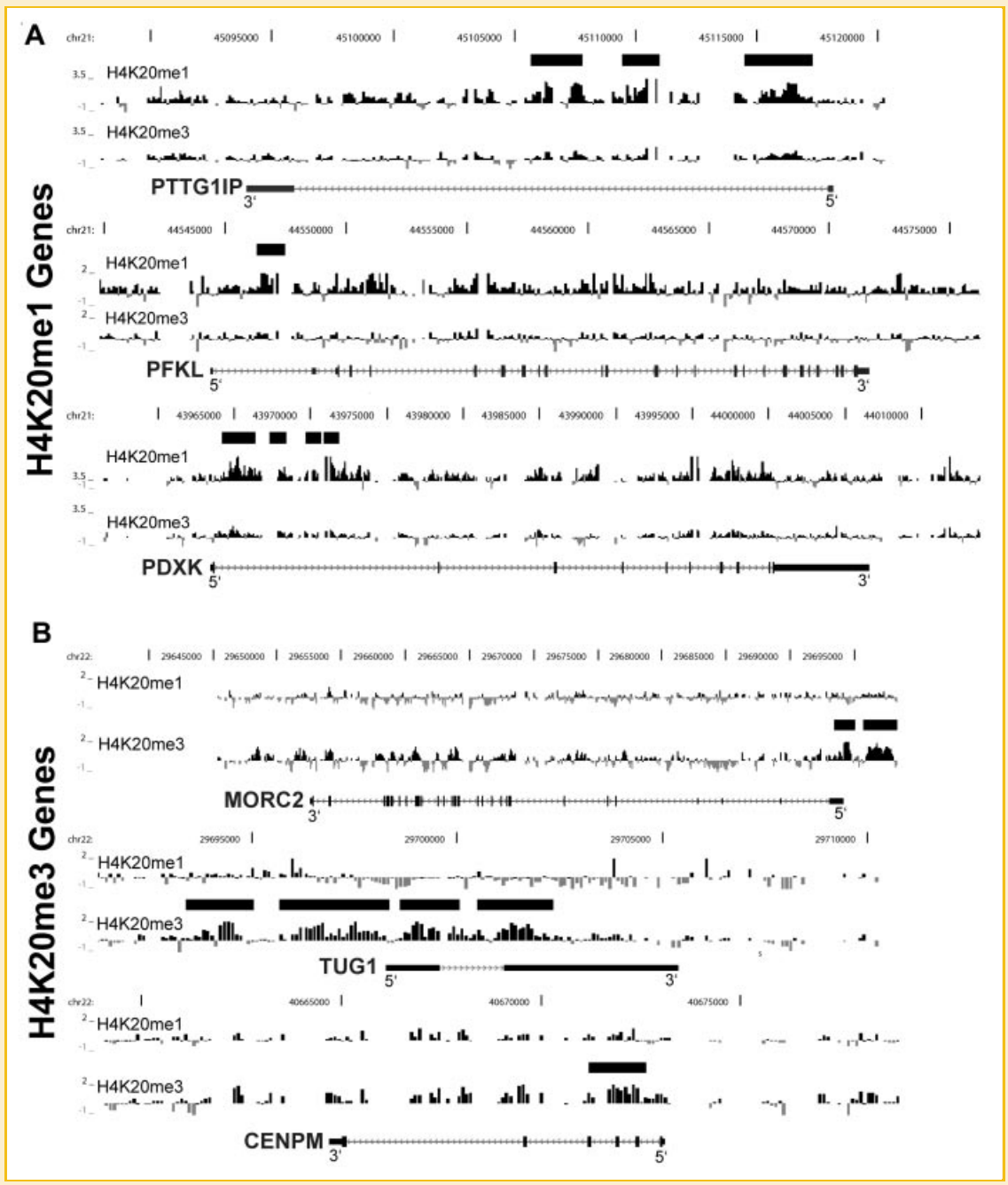

Fig. 2. Identification of H4K20me1- and H4K20me3-associated genes. Three representative H4K20me1-associated genes (A) and H4K20me3-associated genes (B) identified by ChIP-chip are shown. The log 2 ratios of the H4K20me1 and H4K20me3 ChIP-chip data (*y*-axis) were mapped to human chromosomes 21 and 22 (*x*-axis) using the UCSC genome browser. Enrichment of H4K20me1 (top track) and H4K20me3 (bottom track) ChIP DNA compared to input DNA is shown. The large black boxes above the tracks indicate statistically significant ($P < 0.001$) peaks for H4K20me1 or H4K20me3.

distinct genes. By analyzing the most confident sets of genes ($P < 0.001$), our findings indicate that the majority of total genes identified contain either H4K20me1 or H4K20me3 but not both simultaneously (87); only 34 genes over two entire chromosomes contain both modifications. Direct visualization of the ChIP-chip data for these H4K20me1- and H4K20me3-associated genes confirmed these analyses. For genes enriched in H4K20me1, the MA2C program did not generally detect significant peaks of enrichment for H4K20me3 (Fig. 2A). Similarly, significant peaks of H4K20me1 enrichment were not typically detected in H4K20me3-associated genes (Fig. 2B). Collectively, these results indicate that H4K20me1 and H4K20me3 tend to be targeted to different sets of genes, strongly suggesting that each histone modification is physically and functionally distinct.

DISTRIBUTION OF H4K20me1 AND H4K20me3 ENRICHMENT WITHIN TARGET GENES

The direct visualization of the H4K20me1- and H4K20me3-associated genes implied a specific enrichment pattern for each modification within their respective target genes. For H4K20me1-associated genes, the peaks of enrichment appeared to partition more towards the 5′ end of gene bodies than elsewhere (Fig. 2A). While H4K20me3 peaks also appeared to be enriched within the 5′ end of their target genes, they seemed to localize more within gene promoter regions rather than the bodies of genes (Fig. 2B). To qualitatively test these observations and determine the overall distribution of H4K20me1 and H4K20me3 within their target genes, the cumulative peak density for each position in the gene body and the proximal regions (5 kb upstream and downstream) were calculated from all statistically significant ($P < 0.005$) gene targets. The peak densities in the proximal regions were plotted according to single-nucleotide position, whereas the peak densities in the gene body were plotted as percentiles to account for variable gene lengths. Using this approach, we observed that the average gene distribution of H4K20me1 and H4K20me3 were markedly different (Fig. 3). While H4K20me1 appeared to be underrepresented in gene promoters, it seemed to be greatly enriched within the first 5–25% of gene bodies. In contrast, H4K20me3 visually peaked prior to transcription start but did not display any defined enrichment through the length of the gene body.

To provide statistical significance to these observations, the average peak density across the entire region was determined (gray line) and a Poisson distribution model was used to calculate significantly ($P < 0.05$) enriched H4K20me1 and H4K20me3 gene regions (Fig. 3; black bars). Consistent with our visual observations, the analysis indicates that H4K20me3 enrichment was significantly detected from −1306 to −800 relative to transcription start but was not significantly distributed elsewhere within the genes. The analysis also confirmed that H4K20me1 was significantly enriched within the first 6–20% of the gene body; however, the analysis also indicated the presence of another significant region of H4K20me1 enrichment in the center of the gene body (48–51%). Therefore, for H4K20me1-associated genes, our analysis indicates that the majority of H4K20me1 is mainly targeted to the first half of gene bodies with a significant amount of H4K20me1 in the first 25% of the gene. In contrast, for H4K20me3-associated genes, our analysis

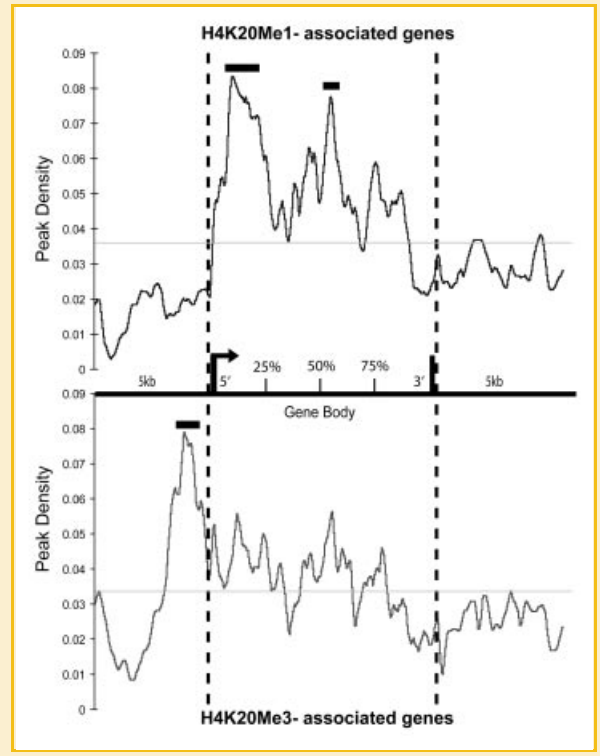

Fig. 3. H4K20me1 is enriched in the first half of gene bodies whereas H4K20me3 is targeted ~1 kb upstream of transcription start. Peak densities of either statistically significant ($P < 0.005$) H4K20me1- or H4K20me3-associated genes were summed (*y*-axis) and plotted as a percentage of the gene body or nucleotide position within the 5 kb proximal regions (*x*-axis). A Poisson distribution was used to determine the average peak density (gray line) and statistically significant ($P < 0.05$) peaks of H4K20me1 and H4K20me3 enrichment (black bars).

indicates that only a small region ~1 kb upstream of transcription start is significantly enriched in H4K20me3. Consistent with the observations above, these differences strongly suggest that H4K20me1 and H4K20me3 are physically distinct histone modifications and have separate functions in transcriptional regulation.

H4K20me1 IS REQUIRED FOR TRANSCRIPTIONAL REPRESSION OF SPECIFIC ENDOGENOUS GENES

Since we had confidently identified a panel of H4K20me1-associated genes, we next sought to determine the role of this histone modification on transcriptional regulation in vivo. Because the PR-Set7/Set8/KMT5a enzyme is the only known H4K20 monomethyltransferase [Fang et al., 2002; Nishioka et al., 2002; Couture et al., 2005; Xiao et al., 2005; Yin et al., 2005], we reasoned that the experimental reduction of PR-Set7 would lead to decreased global levels of H4K20me1 allowing us to determine the resulting effect on the expression of the H4K20me1-associated target genes. First, the basal expression of seven representative H4K20me1-associated genes was determined in wild-type HeLa cells by quantitative real-time PCR (qRT-PCR). The results indicate a wide variation of expression among the different H4K20me1-associated genes ranging from moderate-to-low levels of expression. Next, HeLa cells were transfected with a control shRNA plasmid

or a PR-Set7 shRNA plasmid that depletes cells of PR-Set7 and global levels of H4K20me1 without altering higher degrees of H4K20 methylation (Fig. 4A) [Houston et al., 2008; Sims and Rice, 2008]. To ensure that depletion of PR-Set7 resulted in the local reduction of H4K20me1 at the H4K20me1-associated target genes, ChIPs were performed in the control and PR-Set7 shRNA cells using the H4K20me1-specific antibody, a general histone H3 antibody as the positive control or preimmune rabbit IgG as the negative control. PCR was performed for each sample by using increasing amounts of ChIP template for amplification of two loci within *BRD1* determined to contain significant peaks of H4K20me1 enrichment by ChIP-chip. Our findings demonstrate that, in wild-type cells, H4K20me1 is enriched at the two *BRD1* loci, similar to what we previously observed for *RUNX1* (Fig. 5B) [Sims and Rice, 2008]. While the positive control general H3 amplifications in the control and PR-Set7 shRNA cells were relatively similar, there was a marked reduction of H4K20me1 at both *BRD1* loci in the PR-Set7 shRNA cells confirming a local reduction of H4K20me1. Similar results were observed for H4K20me1-associated regions in *RUNX1* [Sims and Rice, 2008]. These findings demonstrate that depletion of PR-Set7 successfully reduces global and local levels of H4K20me1 at the H4K20me1-associated target gene and, in addition, confirm the previous ChIP-chip experiments in identifying bona fide regions of H4K20me1 enrichment.

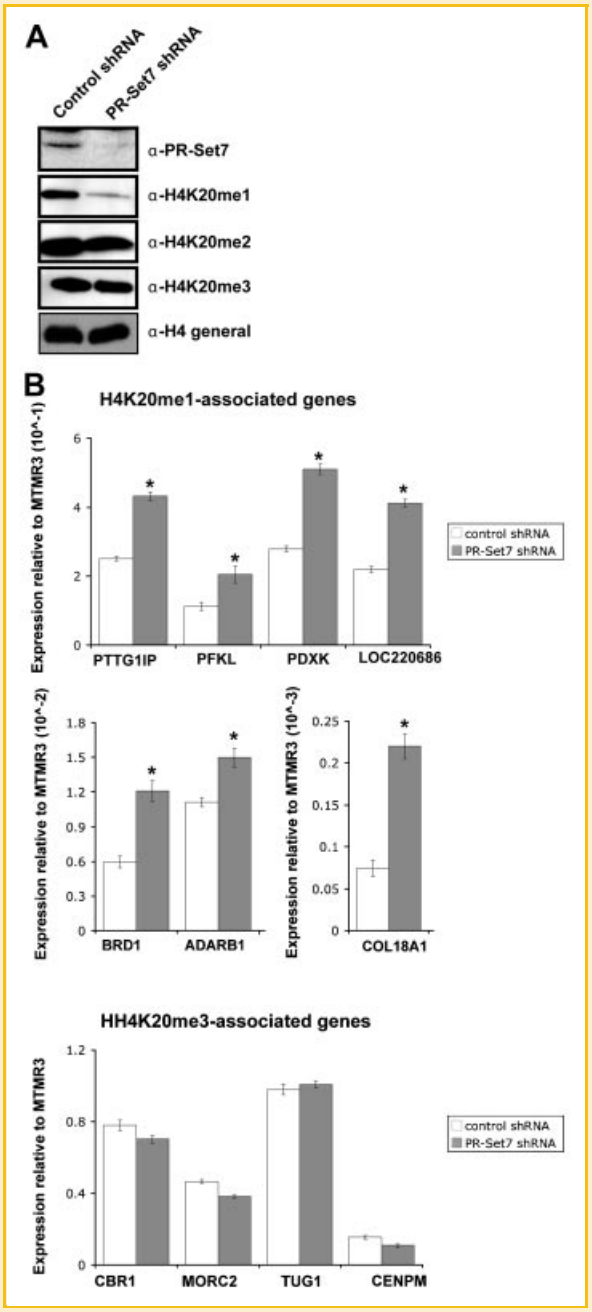

Fig. 4. Depletion of the PR-Set7 H4K20 monomethyltransferase results in the selective derepression of H4K20me1-associated genes. HeLa cells were transfected with a control shRNA plasmid or a PR-Set7 shRNA plasmid. A: Western analysis of whole cell lysates using the indicated antibodies. B: qRT-PCR analysis was performed to analyze the expression levels of seven H4K20me1-associated genes or four H4K20me3-associated genes (C) in cells containing the control shRNA (white) or PR-Set7 shRNA (gray) plasmid. Results are plotted relative to *MTMR3* expression (*y*-axis). Three independent biological replicates were performed to generate the standard deviation in each experiment. The Student's *t*-test was used to determine statistically significant changes at $^{*}P < 0.01$ and $^{**}P < 0.05$.

RNA from the control and PR-Set7 shRNA cells were collected for expression analysis by qRT-PCR. To normalize expression changes between the different samples, several expressed genes were identified on chromosomes 21 and 22 that lacked both H4K20me1 and H4K20me3 (Supplemental Fig. 3). While the expression of these genes, including *MTMR3*, was unaltered, the absence of PR-Set7 and H4K20me1 in the PR-Set7 shRNA cells resulted in a consistent ~2-fold increase in expression of all seven H4K20me1-associated genes regardless of their basal expression status (Fig. 4B). Importantly, the lack of PR-Set7 and H4K20me1 had no detectable effect on the expression of a panel of H4K20me3-associated genes (Fig. 4C). In addition, gene expression changes in several different housekeeping genes were not observed between the different samples (Supplemental Fig. 1).

Since both PR-Set7 and H4K20me1 were reduced in the PR-Set7 shRNA cells, it remained unclear whether PR-Set7 and/or H4K20me1 were directly responsible for the observed repressive effects. To resolve this, HeLa cells were transfected with a control expression plasmid or an expression plasmid containing the sequence of a catalytically dead point mutant of PR-Set7 (CD) that creates a dominant negative phenotype by reducing global levels of H4K20me1 without reducing PR-Set7 (Fig. 5A) [Houston et al., 2008; Sims and Rice, 2008]. To ensure that the PR-Set7 CD plasmid was also reducing H4K20me1 at the target genes, ChIPs were performed as described above. Analogous to the PR-Set7 shRNA cells, there was a marked reduction of H4K20me1 at both *BRD1* H4K20me1 positive regions in the PR-Set7 CD cells indicating that the PR-Set7 CD plasmid induces the local reduction of H4K20me1 (Fig. 5B). Furthermore, ChIP analysis at these regions performed in cells expressing either a wild-type PR-Set7 or the PR-Set7 CD plasmid indicates that both are selectively targeted to these loci (Supplemental Fig. 2). Similar results were observed for *RUNX1* [Sims and Rice, 2008]. The RNA from these cells was collected for expression analysis by qRT-PCR. Strikingly similar to the PR-Set7 shRNA results, the PR-Set7 CD cells consistently displayed an

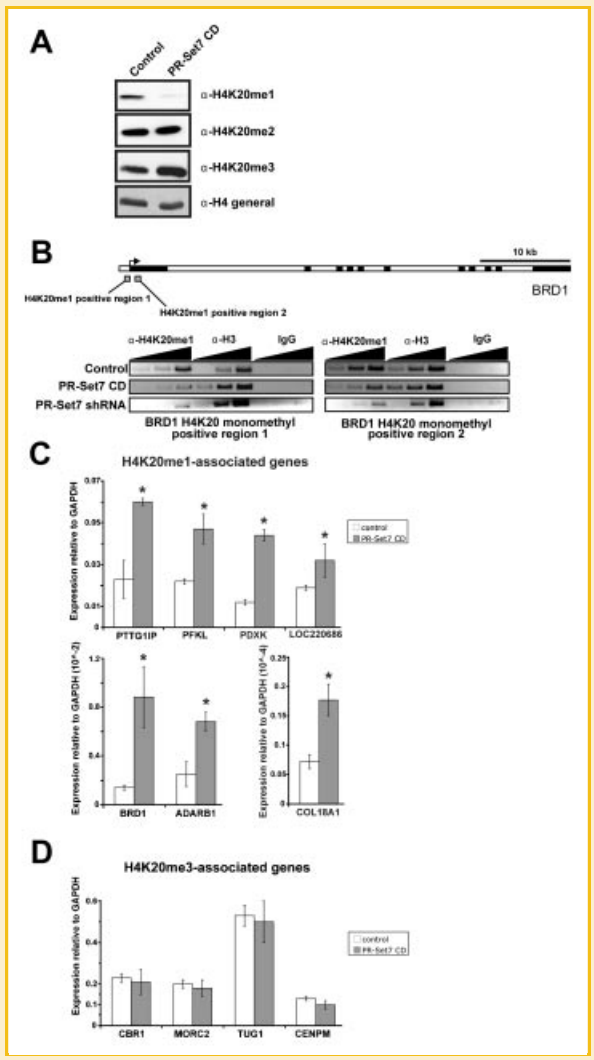

Fig. 5. H4K20me1 is essential for repression of endogenous H4K20me1-associated genes. HeLa cells were transfected with a control eukaryotic plasmid or a plasmid expressing a catalytically dead (CD) dominant negative PR-Set7 point mutant. A: Western analysis of whole cell lysates using the indicated antibodies. B: ChIPs were performed on the HeLa cells transfected with a control (top), a PR-Set7 CD (middle), or a PR-Set7 shRNA expression plasmid (bottom) using either the H4K20me1-specific antibody, a histone H3 general antibody (positive control), or rabbit IgG (negative control). Thirty cycles of PCR amplifications were performed each time for the two H4K20me1 positive regions of *BRD1* using 0.1, 1, or 3 μl of ChIPed DNA from each sample (triangle). C: qRT-PCR analysis was performed to analyze the expression levels of seven H4K20me1-associated genes or four H4K20me3-associated genes (D) in cells expressing the control (white) or PR-Set7 CD (gray) plasmid. Results are plotted relative to *MTMR3* expression (*y*-axis). Three independent biological replicates were performed to generate the standard deviation in each experiment. The Student's *t*-test was used to determine statistically significant changes at $^{*}P < 0.01$.

~2-fold increase in the expression of all seven H4K20me1-associated genes when compared to control (Fig. 5C). No changes in the expression of the four H4K20me3-associated genes were detected in the PR-Set7 CD cells (Fig. 5D). Collectively, these findings indicate that PR-Set7 and H4K20me1 are targeted to specific genes to directly participate in a transcriptionally repressive program; a biological program that is functionally distinct from H4K20me3.

SPECIFIC GENOMIC SEQUENCES RECRUIT H4K20me1 TO INDUCE REPRESSION

Our findings above indicate that H4K20me1 is targeted to the first half of gene bodies and the modification, itself, plays an essential role in transcriptional repression of specific sets of genes. Based on these observations, we hypothesized that the DNA sequences significantly enriched in H4K20me1 function as enhancer elements and that H4K20me1 serves to repress their transcriptional enhancer function. To determine if these elements contained enhancer functions, we cloned several H4K20me1-associated DNA sequences into the pTK-luc2 reporter vector where each insert was located just 5′ of a minimal TK promoter that drives constitutive luciferase expression [Wen et al., 1999]. Contrary to our hypothesis, transfection of these constructs into HEK 293 cells revealed that all H4K20me1-associated DNA sequences significantly reduced basal TK promoter activity, rather than enhancing it, as illustrated by the massive reductions in luciferase expression for each construct compared to the pTK-luc2 control (Fig. 6A). In contrast, a sequence corresponding to an H4K20me1-negative region within *RUNX1* failed to alter luciferase expression indicating that the repressive effects were specific to the H4K20me1-associated DNA sequences. To exclude the possibility that the repressive effect was restricted to

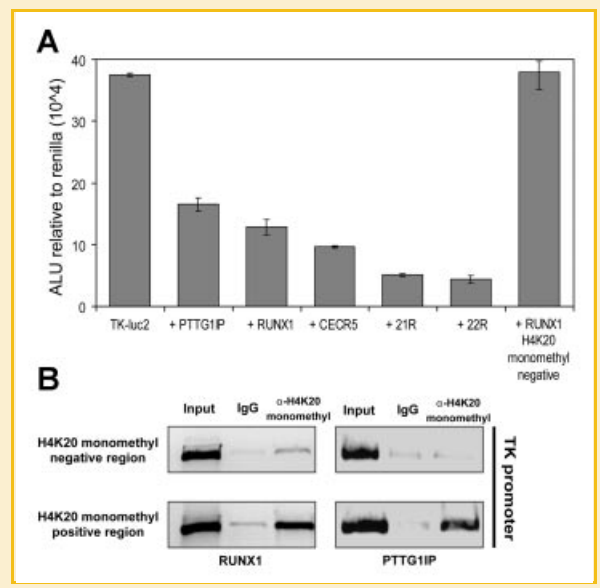

Fig. 6. Specific genomic sequences recruit H4K20me1 to induce repression. A: The H4K20me1-positive sequences from *PTTG1IP*, *RUNX1*, *CECR5* and regions on chromosomes 21 and 22 (21R and 22R) and an H4K20me1-negative region from *RUNX1* were individually cloned into the pTK-luc2 reporter vector and transfected into HEK 293 cells. The arbitrary light units (ALU) from the luciferase assays were normalized by co-transfection with the pRL-CMV vector (*y*-axis). Three independent experiments were performed to generate standard deviation. B: ChIPs were performed on the HEK 293 cells transfected with the pTK-luc2 vectors containing the *RUNX1* and *PTTG1IP* H4K20me1 positive and negative regions using the H4K20me1-specific antibody or rabbit IgG as the negative control. Comparative analysis between the samples was possible due to the equal PCR amplification of the input materials.

regions within genes, we performed similar experiments using H4K20me1-associated DNA sequences far outside of genes in both chromosomes 21 and 22 (21R and 22R, respectively). In both cases, luciferase expression was greatly reduced compared to control. These findings indicate that the H4K20me1-associated DNA sequences are inherently repressive regardless of genomic location.

The findings above suggest that the DNA sequences nucleate the monomethylation of H4K20 to induce repression. To test this, ChIPs were performed on the HEK 293 cells transfected with the pTK-luc2 vector containing either the *RUNX1* H4K20me1 positive or negative region. PCR amplifications of the ChIPed material were performed using primers that specifically amplify the minimal TK promoter. Consistent with our hypothesis, our results indicate that the *RUNX1* H4K20me1-associated sequence was selectively monomethylated compared to the *RUNX1* negative sequence when normalized to the PCR amplifications of the input ChIP material (Fig. 6B). Similar results were obtained when testing a PTTG1IP H4K20me1 positive DNA sequence and a negative DNA sequence. These results demonstrate that specific genomic sequences are sufficient for the nucleation of H4K20me1 and transcriptional repression in vivo.

DISCUSSION

We previously demonstrated that H4K20me1 and H4K20me3 are compartmentalized to distinct regions of silent chromatin [Sims et al., 2006]. In this study we sought to expand on these observations by employing ChIP-chip to define the precise genomic locations of H4K20me1 and H4K20me3 across human chromosomes 21 and 22. By using the MA2C peak-calling program that assigns statistical significance to the data, we were able to confidently identify and verify peaks and genes enriched in H4K20me1 or H4K20me3. Subsequent analysis revealed that H4K20me1 is typically excluded from repetitive elements but preferentially enriched within the bodies of specific genes; typically within the first half of the gene body. The distribution of H4K20me1 in genes is consistent with recent findings using high-throughput next generation sequencing of ChIPed material (ChIP-Seq) [Barski et al., 2007; Cui et al., 2009; Rosenfeld et al., 2009].

In contrast to H4K20me1, our analysis indicates that H4K20me3 is largely targeted to repetitive elements. These findings are consistent with a previous study using ChIP in conjunction with microarrays containing common classes of mouse repetitive elements [Martens et al., 2005]. While they detected H4K20me3 enrichment preferentially at major and minor satellite repeats and LTRs in mouse embryonic stem cells, our ChIP-cloning findings from HeLa cells suggest that H4K20me3 is preferentially targeted to SINE elements in humans rather than satellite repeats or LTRs. The discrepancy of these findings is likely due to differences in technical approaches and/or species studied. Although both findings indicate that H4K20me3 is preferentially targeted to repetitive elements, we were also able to identify a new panel of genes on human chromosomes 21 and 22 that contained peaks of H4K20me3 enrichment. In contrast to H4K20me1, the H4K20me3 peaks appeared to be targeted to a small region ~1 kb upstream of transcription start. This gene-specific enrichment of H4K20me3 has not been previously observed [Barski et al., 2007]. While our findings strongly imply a role for H4K20me3 in transcription regulation, the biological significance of H4K20me3 in the 5′ regulatory region of specific genes remains unknown.

It was originally reported that H4K20me1 was associated with transcriptionally repressed chromatin [Fang et al., 2002; Nishioka et al., 2002; Kohlmaier et al., 2004; Karachentsev et al., 2005; Sims et al., 2006]. However, subsequent studies by others demonstrated that H4K20me1 was found within actively transcribed genes, suggesting a role for H4K20me1 in gene activation [Talasz et al., 2005; Vakoc et al., 2006]. Since our ChIP-chip analysis had identified a novel panel of genes specifically enriched in H4K20me1, we sought to use these genes in order to clarify the role H4K20me1 in transcription. By employing RNAi for PR-Set7 to reduce global and local levels of H4K20me1, we observed a consistent ~2-fold increase in the expression of all H4K20me1-associated genes examined; expression changes for H4K20me3-associated genes were not detected. Similarly, by employing a dominant negative catalytically dead point mutant of PR-Set7, we observed the same ~2-fold increase in expression of the H4K20me1-associated genes. These findings clearly indicate that a major role of H4K20me1, itself, is in the transcriptional repression of specific genes.

Our findings demonstrate that the repressive effects of H4K20me1 appear to function non-discriminately between H4K20me1-associated genes that are actively transcribed or silenced. A wide variation in the basal expression levels of the different H4K20me1-associated genes was observed in wild-type cells; however, when H4K20me1 was depleted, all genes increased their transcriptional output by ~2-fold. These findings imply a novel role for H4K20me1 in regulating gene dosage whereby one allele of an H4K20me1-associated gene could be transcriptionally active while the other, containing H4K20me1, could be repressed. Therefore, a reduction in H4K20me1 would result in derepression of this allele and an ~2-fold increase in overall gene expression, as we observed for all H4K20me1-associated genes examined. Consistent with this gene dosing theory, H4K20me1 is enriched on the mammalian inactive X chromosome and, therefore, may play a role in dosage compensation [Kohlmaier et al., 2004; Sims et al., 2006]. Although the H4K20me1 gene-dosing model may function at specific genes, it does not appear to function at imprinted loci: a recent study examining the mouse H19 imprinting control region detected H4K20me1 on both the paternal and maternal alleles [Pannetier et al., 2008].

Recent findings have contributed important insights into how H4K20me1 mediates gene repression. Increasing evidence indicates that histone modifications can recruit and bind a conserved motif within specific regulatory proteins to initiate and/or maintain a specific DNA-templated process [Jenuwein and Allis, 2001]. Consistent with this, recent reports demonstrated that one of the three conserved *m*alignant *b*rain *t*umor (MBT) domains of the transcriptional repressor protein L3MBTL1 preferentially binds the mono- and dimethylated forms of H4K20 [Li et al., 2007; Min et al., 2007]. Subsequent studies demonstrated that H4K20me1 was required for the recruitment and induction of L3MBTL1's repressive effects of a stable reporter gene in vivo [Kalakonda et al., 2008]. Furthermore, the depletion of L3MBTL1 resulted in the derepression of endogenous H4K20me1-associated genes including *RUNX1* and

c-myc [Trojer et al., 2007; Sims and Rice, 2008]. The binding of L3MBTL1 to H4K20me1-containing nucleosome arrays resulted in chromatin condensation, thereby, creating a physical barrier to transcription [Trojer et al., 2007]. These findings suggest that L3MBTL1 is recruited to the H4K20me1-associated genes identified in this study; however, further investigations are required to determine this.

Importantly, we demonstrated that the H4K20me1-associated DNA fragments were sufficient to recruit H4K20 methylation and induce the repression of a reporter gene. These findings indicate that the DNA sequences, themselves, are a critical upstream component of the H4K20me1 repressive pathway. Collectively, our findings suggest that the specific DNA sequences recruit PR-Set7 to monomethylate H4K20 which, in turn, recruits and binds L3MBTL1 to induce chromatin condensation and transcriptional repression. Current investigations are underway to test this model. While this model predicts the existence of a putative consensus sequence for PR-Set7 recruitment, our initial examinations have failed to identify one; this is on-going. However, it is likely that a consensus sequence exists since the DNA sequences that recruit H4K20me1 tend to be found in regions that are evolutionarily conserved; further studies are in progress to determine this. Since these sequences and the PR-Set7 H4K20 monomethyltransferase are conserved, it is also likely that this pathway regulates gene transcription of similar sets of genes in other multicellular eukaryotes including metazoans and chordates [Karachentsev et al., 2005; Spada et al., 2005].

Previous reports postulated that the Suv4-20 methyltransferases used H4K20me1 as its preferred substrate to di- and trimethylate H4K20, as the depletion of the Suv4-20 enzymes resulted in dramatically elevated levels of H4K20me1 [Schotta et al., 2008; Yang et al., 2008]. Similarly, several recent reports demonstrated that the loss of PR-Set7 and H4K20me1 resulted in a concomitant reduction of H4K20me2 and H4K20me3 consistent with the model that H4K20me1 is the preferred substrate for higher degrees of H4K20 methylation [Tardat et al., 2007; Pannetier et al., 2008; Oda et al., 2009]. In contrast to these findings, we observed no detectable changes in H4K20me2 and H4K20me3 in various human cell lines lacking PR-Set7 and H4K20me1 [Sims et al., 2006; Houston et al., 2008; Sims and Rice, 2008]. The reasons for the differences remain unclear and further experimentation will be required to resolve the numerous possibilities that could account for the differences. However, by concurrently investigating the precise genomic localizations of H4K20me1 and H4K20me3, our findings strongly suggest that these two histone modifications are physically and functionally distinct. The ChIP-cloning and ChIP-chip findings indicate that H4K20me1 and H4K20me3 are preferentially localized to different genomic regions: gene bodies or repetitive elements, respectively. Identification of genes enriched in the different degrees of H4K20 methylation revealed that the majority of these genes contained either H4K20me1 or H4K20me3, but not both modifications simultaneously. Furthermore, the average peak distribution of H4K20me1 and H4K20me3 in gene regions was dramatically different: the first half of gene bodies or 5′ regulatory region, respectively. Collectively, our findings strongly suggest that higher degrees of H4K20 methylation are not completely dependent upon the prior monomethylation of H4K20 by PR-Set7.

ACKNOWLEDGMENTS

We thank Axel Schonthal and Baruch Frenkel for discussion and for the pTK2-luc2 plasmid. J.C.R. is a Pew Scholar in the Biomedical Sciences and is partially supported by the National Institutes of Health (GM075094). S.I.H. was partially supported by a grant from the California Breast Cancer Research Program. We also thank The Donald E. and Delia B. Baxter Foundation and The Robert E. and May R. Wright Foundation for their generous support.

REFERENCES

Barski A, Cuddapah S, Cui K, Roh TY, Schones DE, Wang Z, Wei G, Chepelev I, Zhao K. 2007. High-resolution profiling of histone methylations in the human genome. Cell 129:823–837.

Bernstein BE, Kamal M, Lindblad-Toh K, Bekiranov S, Bailey DK, Huebert DJ, McMahon S, Karlsson EK, Kulbokas EJ III, Gingeras TR, Schreiber SL, Lander ES. 2005. Genomic maps and comparative analysis of histone modifications in human and mouse. Cell 120:169–181.

Botuyan MV, Lee J, Ward IM, Kim JE, Thompson JR, Chen J, Mer G. 2006. Structural basis for the methylation state-specific recognition of histone H4-K20 by 53BP1 and Crb2 in DNA repair. Cell 127:1361–1373.

Boyer LA, Lee TI, Cole MF, Johnstone SE, Levine SS, Zucker JP, Guenther MG, Kumar RM, Murray HL, Jenner RG, Gifford DK, Melton DA, Jaenisch R, Young RA. 2005. Core transcriptional regulatory circuitry in human embryonic stem cells. Cell 122:947–956.

Boyer LA, Plath K, Zeitlinger J, Brambrink T, Medeiros LA, Lee TI, Levine SS, Wernig M, Tajonar A, Ray MK, Bell GW, Otte AP, Vidal M, Gifford DK, Young RA, Jaenisch R. 2006. Polycomb complexes repress developmental regulators in murine embryonic stem cells. Nature 441:349–353.

Couture JF, Collazo E, Brunzelle JS, Trievel RC. 2005. Structural and functional analysis of SET8, a histone H4 Lys-20 methyltransferase. Genes Dev 19:1455–1465.

Cui K, Zang C, Roh TY, Schones DE, Childs RW, Peng W, Zhao K. 2009. Chromatin signatures in multipotent human hematopoietic stem cells indicate the fate of bivalent genes during differentiation. Cell Stem Cell 4:80–93.

Fang J, Feng Q, Ketel CS, Wang H, Cao R, Xia L, Erdjument-Bromage H, Tempst P, Simon JA, Zhang Y. 2002. Purification and functional characterization of SET8, a nucleosomal histone H4-lysine 20-specific methyltransferase. Curr Biol 12:1086–1099.

Guenther MG, Levine SS, Boyer LA, Jaenisch R, Young RA. 2007. A chromatin landmark and transcription initiation at most promoters in human cells. Cell 130:77–88.

Heintzman ND, Stuart RK, Hon G, Fu Y, Ching CW, Hawkins RD, Barrera LO, Van Calcar S, Qu C, Ching KA, Wang W, Weng Z, Green RD, Crawford GE, Ren B. 2007. Distinct and predictive chromatin signatures of transcriptional promoters and enhancers in the human genome. Nat Genet 39:311–318.

Houston SI, McManus KJ, Adams MM, Sims JK, Carpenter PB, Hendzel MJ, Rice JC. 2008. Catalytic function of the PR-Set7 histone H4 lysine 20 monomethyltransferase is essential for mitotic entry and genomic stability. J Biol Chem 283:19478–19488.

Huen MS, Sy SM, van Deursen JM, Chen J. 2008. Direct interaction between SET8 and PCNA couples H4-K20 methylation with DNA replication. J Biol Chem 283:11073–11077.

Jenuwein T, Allis CD. 2001. Translating the histone code. Science 293:1074–1080.

Jorgensen S, Elvers I, Trelle MB, Menzel T, Eskildsen M, Jensen ON, Helleday T, Helin K, Sorensen CS. 2007. The histone methyltransferase SET8 is required for S-phase progression. J Cell Biol 179:1337–1345.

Kalakonda N, Fischle W, Boccuni P, Gurvich N, Hoya-Arias R, Zhao X, Miyata Y, Macgrogan D, Zhang J, Sims JK, Rice JC, Nimer SD. 2008. Histone

H4 lysine 20 monomethylation promotes transcriptional repression by L3MBTL1. Oncogene 27:4293–4304.

Karachentsev D, Sarma K, Reinberg D, Steward R. 2005. PR-Set7-dependent methylation of histone H4 Lys 20 functions in repression of gene expression and is essential for mitosis. Genes Dev 19:431–435.

Karolchik D, Kuhn RM, Baertsch R, Barber GP, Clawson H, Diekhans M, Giardine B, Harte RA, Hinrichs AS, Hsu F, Kober KM, Miller W, Pedersen JS, Pohl A, Raney BJ, Rhead B, Rosenbloom KR, Smith KE, Stanke M, Thakkapallayil A, Trumbower H, Wang T, Zweig AS, Haussler D, Kent WJ. 2008. The UCSC Genome Browser Database: 2008 update. Nucleic Acids Res 36:D773–D779.

Kohlmaier A, Savarese F, Lachner M, Martens J, Jenuwein T, Wutz A. 2004. A chromosomal memory triggered by Xist regulates histone methylation in X inactivation. PLoS Biol 2:E171.

Kuo MH, Allis CD. 1999. In vivo cross-linking and immunoprecipitation for studying dynamic protein:DNA associations in a chromatin environment. Methods 19:425–433.

Li H, Fischle W, Wang W, Duncan EM, Liang L, Murakami-Ishibe S, Allis CD, Patel DJ. 2007. Structural basis for lower lysine methylation state-specific readout by MBT repeats of L3MBTL1 and an engineered PHD finger. Mol Cell 28:677–691.

Martens JH, O'Sullivan RJ, Braunschweig U, Opravil S, Radolf M, Steinlein P, Jenuwein T. 2005. The profile of repeat-associated histone lysine methylation states in the mouse epigenome. EMBO J 24:800–812.

Mikkelsen TS, Ku M, Jaffe DB, Issac B, Lieberman E, Giannoukos G, Alvarez P, Brockman W, Kim TK, Koche RP, Lee W, Mendenhall E, O'Donovan A, Presser A, Russ C, Xie X, Meissner A, Wernig M, Jaenisch R, Nusbaum C, Lander ES, Bernstein BE. 2007. Genome-wide maps of chromatin state in pluripotent and lineage-committed cells. Nature 448:553–560.

Min J, Allali-Hassani A, Nady N, Qi C, Ouyang H, Liu Y, MacKenzie F, Vedadi M, Arrowsmith CH. 2007. L3MBTL1 recognition of mono- and dimethylated histones. Nat Struct Mol Biol 14:1229–1230.

Murray K. 1964. The occurrence of e-N-methyl lysine in histones. Biochemistry 3:10–15.

Nelson JD, Denisenko O, Sova P, Bomsztyk K. 2006. Fast chromatin immunoprecipitation assay. Nucleic Acids Res 34:e2.

Nishioka K, Rice JC, Sarma K, Erdjument-Bromage H, Werner J, Wang Y, Chuikov S, Valenzuela P, Tempst P, Steward R, Lis JT, Allis CD, Reinberg D. 2002. PR-Set7 is a nucleosome-specific methyltransferase that modifies lysine 20 of histone H4 and is associated with silent chromatin. Mol Cell 9:1201–1213.

Oda H, Okamoto I, Murphy N, Chu J, Price SM, Shen MM, Torres-Padilla ME, Heard E, Reinberg D. 2009. Monomethylation of histone H4-lysine 20 is involved in chromosome structure and stability and is essential for mouse development. Mol Cell Biol 29:2278–2295.

Pannetier M, Julien E, Schotta G, Tardat M, Sardet C, Jenuwein T, Feil R. 2008. PR-SET7 and SUV4-20H regulate H4 lysine-20 methylation at imprinting control regions in the mouse. EMBO Rep 9:998–1005.

Pesavento JJ, Yang H, Kelleher NL, Mizzen CA. 2007. Certain and progressive methylation of histone H4 at lysine 20 during the cell cycle. Mol Cell Biol 28:468–486.

Rice JC, Nishioka K, Sarma K, Steward R, Reinberg D, Allis CD. 2002. Mitotic-specific methylation of histone H4 Lys 20 follows increased PR-Set7 expression and its localization to mitotic chromosomes. Genes Dev 16:2225–2230.

Rosenfeld JA, Wang Z, Schones DE, Zhao K, DeSalle R, Zhang MQ. 2009. Determination of enriched histone modifications in non-genic portions of the human genome. BMC Genomics 10:143.

Sakaguchi A, Steward R. 2007. Aberrant monomethylation of histone H4 lysine 20 activates the DNA damage checkpoint in Drosophila melanogaster. J Cell Biol 176:155–162.

Sakaguchi A, Karachentsev D, Seth-Pasricha M, Druzhinina M, Steward R. 2008. Functional characterization of the *Drosophila* Hmt4-20/Suv 4-20 histone methyltransferase. Genetics 179:317–322.

Sanders SL, Portoso M, Mata J, Bahler J, Allshire RC, Kouzarides T. 2004. Methylation of histone H4 lysine 20 controls recruitment of Crb2 to sites of DNA damage. Cell 119:603–614.

Sautel CF, Cannella D, Bastien O, Kieffer S, Aldebert D, Garin J, Tardieux I, Belrhali H, Hakimi MA. 2007. SET8-mediated methylations of histone H4 lysine 20 mark silent heterochromatic domains in apicomplexan genomes. Mol Cell Biol 27:5711–5724.

Schotta G, Lachner M, Sarma K, Ebert A, Sengupta R, Reuter G, Reinberg D, Jenuwein T. 2004. A silencing pathway to induce H3-K9 and H4-K20 trimethylation at constitutive heterochromatin. Genes Dev 18:1251–1262.

Schotta G, Sengupta R, Kubicek S, Malin S, Kauer M, Callen E, Celeste A, Pagani M, Opravil S, De La Rosa-Velazquez IA, Espejo A, Bedford MT, Nussenzweig A, Busslinger M, Jenuwein T. 2008. A chromatin-wide transition to H4K20 monomethylation impairs genome integrity and programmed DNA rearrangements in the mouse. Genes Dev 22:2048–2061.

Sims JK, Rice JC. 2008. PR-Set7 establishes a repressive trans-tail histone code that regulates differentiation. Mol Cell Biol 28:4459–4468.

Sims JK, Houston SI, Magazinnik T, Rice JC. 2006. A trans-tail histone code defined by monomethylated H4 Lys-20 and H3 Lys-9 demarcates distinct regions of silent chromatin. J Biol Chem 281:12760–12766.

Song JS, Johnson WE, Zhu X, Zhang X, Li W, Manrai AK, Liu JS, Chen R, Liu XS. 2007. Model-based analysis of two-color arrays (MA2C). Genome Biol 8:R178.

Spada F, Chioda M, Thompson EM. 2005. Histone H4 post-translational modifications in chordate mitotic and endoreduplicative cell cycles. J Cell Biochem 95:885–901.

Strahl BD, Allis CD. 2000. The language of covalent histone modifications. Nature 403:41–45.

Talasz H, Lindner HH, Sarg B, Helliger W. 2005. Histone H4-lysine 20 monomethylation is increased in promoter and coding regions of active genes and correlates with hyperacetylation. J Biol Chem 280:38814–38822.

Tardat M, Murr R, Herceg Z, Sardet C, Julien E. 2007. PR-Set7-dependent lysine methylation ensures genome replication and stability through S phase. J Cell Biol 179:1413–1426.

Trojer P, Li G, Sims RJ III, Vaquero A, Kalakonda N, Boccuni P, Lee D, Erdjument-Bromage H, Tempst P, Nimer SD, Wang YH, Reinberg D. 2007. L3MBTL1, a histone-methylation-dependent chromatin lock. Cell 129:915–928.

Vakoc CR, Sachdeva MM, Wang H, Blobel GA. 2006. Profile of histone lysine methylation across transcribed mammalian chromatin. Mol Cell Biol 26: 9185–9195.

Weinmann AS, Farnham PJ. 2002. Identification of unknown target genes of human transcription factors using chromatin immunoprecipitation. Methods 26:37–47.

Wen X, Lin HH, Shih HM, Kung HJ, Ann DK. 1999. Kinase activation of the non-receptor tyrosine kinase Etk/BMX alone is sufficient to transactivate STAT-mediated gene expression in salivary and lung epithelial cells. J Biol Chem 274:38204–38210.

Xiao B, Jing C, Kelly G, Walker PA, Muskett FW, Frenkiel TA, Martin SR, Sarma K, Reinberg D, Gamblin SJ, Wilson JR. 2005. Specificity and mechanism of the histone methyltransferase Pr-Set7. Genes Dev 19:1444–1454.

Yang H, Mizzen CA. 2009. The multiple facets of histone H4-lysine 20 methylation. Biochem Cell Biol 87:151–161.

Yang H, Pesavento JJ, Starnes TW, Cryderman DE, Wallrath LL, Kelleher NL, Mizzen CA. 2008. Preferential dimethylation of histone H4-lysine 20 by Suv 4-20. J Biol Chem 283:12085–12092.

Yin Y, Liu C, Tsai SN, Zhou B, Ngai SM, Zhu G. 2005. SET8 recognizes the sequence RHRK20VLRDN within the N terminus of histone H4 and monomethylates lysine 20. J Biol Chem 280:30025–30031.